Monthly Notices
of the
ROYAL ASTRONOMICAL SOCIETY

MNRAS **455,** 3991–3999 (2016) doi:10.1093/mnras/stv2555

Observational aspects of galactic accretion at redshift 3.3

Michael Rauch,[1]★ George D. Becker[2] and Martin G. Haehnelt[3]

[1]*Carnegie Observatories, 813 Santa Barbara Street, Pasadena, CA 91101, USA*
[2]*Department of Physics & Astronomy, University of California, Riverside, 900 University Ave, Riverside, CA 92521, USA*
[3]*Institute of Astronomy and Kavli Institute for Cosmology, Cambridge University, Madingley Road, Cambridge CB30HA, UK*

Accepted 2015 October 28. Received 2015 October 28; in original form 2015 September 25

ABSTRACT

We investigate the origin of extragalactic continuum emission and its relation to the stellar population of a recently discovered peculiar $z = 3.344$ Ly α emitter. Based on an analysis of the broad-band colours and morphology, we find further support for the idea that the underlying galaxy is being fed by a large-scale ($L \geq 35$ kpc) accretion stream. Archival*HST* images show small-scale ($\sim$5 kpc) tentacular filaments converging near a hotspot of star formation, possibly fueled by gas falling in along the filaments. The spectral energy distribution of the tentacles is broadly compatible with either (1) non-ionizing rest-frame far-UV continuum emission from stars formed in a 60 million-year-old starburst; (2) nebular two-photon continuum radiation, arising from collisional excitation cooling; or (3) a recombination spectrum emitted by hydrogen fluorescing in response to ionizing radiation escaping from the galaxy. The latter possibility simultaneously accounts for the presence of asymmetric Lyα emission from the large-scale gaseous filament, and the nebular continuum in the smaller scale tentacles as caused by the escape of ionizing radiation from the galaxy. Possible astrophysical explanations for the nature of the tentacles include: a galactic wind powered by the starburst; infalling gas during cold accretion, or tails of interstellar medium dragged out of the galaxy by satellite haloes that have plunged through the main halo. The possibility of detecting extragalactic two-photon continuum emission in space-based, broad-band images suggests a tool for studying the gaseous environment of high-redshift galaxies at much greater spatial detail than possible with Lyα or other resonance line emission.

Key words: galaxies: dwarf – galaxies: evolution – galaxies: interactions – intergalactic medium – dark ages, reionization, first stars – diffuse radiation.

1 INTRODUCTION

Exchanges of gas between galaxies and the ambient intergalactic medium (IGM) are thought to play an important role in the formation of galaxies. Inflows of gas may be the dominant feeding mechanism for most galaxies through most of cosmic time. Outflows of some kind are thought to regulate the galactic baryon/metal budgets, galactic morphology, the shape of the luminosity function and the enrichment of the IGM with metals. Intergalactic gas flows can be detected from the absorption lines they cause in the spectra of background QSOs or bright galaxies. Because of the sparse spatial sampling and the largely statistical nature of such constraints, establishing a unique correspondence between absorption lines and galactic in- or outflows has remained difficult and highly model-dependent. An unambiguous understanding of the nature of intergalactic gas flows requires some form of direct imaging of the spatially extended emission from the galactic gaseous environment.

Taking two-dimensional images of high-redshift gas in emission is most likely to succeed by observing the redshifted H I Lyα emission line, powered by a strong source of ionizing radiation. Thus, most of the detections of extended emission so far are due to fluorescence of Ly α in response to ionizing photons in the vicinity of an active galactic nucleus (AGN; e.g. Fynbo, Møller & Warren 1999; Bunker et al. 2003; Francis & Bland-Hawthorn 2004; Weidinger, Møller & Fynbo 2004; Cantalupo et al. 2005; Adelberger et al. 2006; Cantalupo, Lilly & Porciani 2007; Hennawi et al. 2009; Kollmeier et al. 2010; Trainor & Steidel 2013; Martin et al. 2014a,b, 2015). Extended Ly α emission is also seen among emitters detected in narrow-band imaging surveys without direct reference to the presence of an AGN. At the bright end of the luminosity distribution of these objects, the so-called Ly α blobs are likely to reflect an inhomogeneous population of gaseous haloes lit up by, again, AGN (e.g. Overzier et al. 2013; Prescott et al. 2015, and references therein), strong star formation (e.g. Cen & Zheng 2013; Ouchi et al. 2013; Zabl et al. 2015) cooling of gas falling into gravitational potential wells, (e.g. Haiman, Spaans & Quataert 2000; Fardal et al. 2001) and possibly other feedback processes. The simultaneous

★ E-mail: mr@obs.carnegiescience.edu

association of these processes with the formation of massive haloes so far has made it difficult to disentangle them observationally. Studying the gas/galaxy interface of a more typical, lower mass galaxy one would expect star formation to become the dominant source of Ly α emission, with the main difficulty shifting to being able to detect extended emission related to star-formation rates (SFRs) on the order of a few solar masses per year. For a $z \sim 3$ galaxy, a SFR of 1 $M_\odot$ yr^{-1}, translates into a total, unattenuated Ly α flux (predicted for case B conditions) of 1.4 $\times$ 10^{-17} erg s^{-1} cm^{-2}, about an order of magnitude fainter than Ly α blobs typically uncovered by narrow band surveys (e.g. Matsuda et al. 2004). The higher detection sensitivity required to see extended haloes at such fluxes can be achieved through long exposures and a spectroscopic search strategy as opposed to a traditional narrowband filter survey. Trying to detect Ly α sources (observed through a blindly positioned spectrograph slit) in a 2D spectrum considerably reduces the sky background noise by a factor of $\sqrt{\Delta\lambda_{\rm NB}/\Delta\lambda_{\rm spec}}$, where $\Delta\lambda_{\rm NB}$ is the width of a typical narrow band filter, and $\Delta\lambda_{\rm spec}$ is the spectral resolution element of a typical low-resolution spectrograph. A similar suppression can be achieved by applying a judiciously positioned slice in wavelength space a posteriori through the data cube recorded with an integral field unit (IFU). Such surveys have reached surface brightness limits of 8 $\times$ 10^{-20} erg cm^{-2} s^{-1} arcsec^{-2} per arcsec^2 aperture. At this level many $z \sim 3$ galaxies *individually* show extended Ly α emission, even with SFR less than 1 $M_\odot$ yr^{-1} (Rauch et al. 2008). The brighter ones of those objects exhibit surface brightness profiles best described as a relatively compact core with broad wings (Rauch et al. 2013a, fig. 6), which can be reproduced by simple models of H I haloes, where Ly α photons propagate from a central source through an optically thick H I coccoon (e.g. Dijkstra, Haiman & Spaans 2006; Rauch et al. 2013a, fig. B1). Studies stacking narrowband images of many haloes of individually lower S/N (e.g. Hayashino et al. 2004; Steidel et al. 2011, Feldmeier et al. 2013; Momose et al. 2014) confirm this finding of extended haloes in an average sense, but suggest that the ensemble properties of the extended haloes are sensitive to the sample selection criteria (e.g. broad-band-selected versus narrowband selected), and to the redshift.

Among the individually extended haloes found in our earlier searches, there is a subset of widely extended (several tens of kpc wide), Ly α haloes, whose surface brightness profiles do not exhibit the spatial symmetry or the rapid drop commonly found among Ly α emitting galaxies. These objects include haloes with vaguely filamentary extensions, apparently corresponding to infalling gas and satellites (Rauch et al. 2011, 2013a, 2014), and in one case, a candidate for starformation triggered by external AGN feedback (Rauch et al. 2013b). As these cases are rare relative to the more common spatially symmetric and compact Ly α emitters, it appears that they represent phases in the formation of galactic haloes, where short-lived phenomena like starbursts or AGN activity briefly light up the distant gaseous surroundings of high z galaxies.

In this paper, we revisit one of these objects, the peculiar extended and asymmetric $z = 3.344$ Ly α emitter related to a galaxy at position 03:32:38.815, −27:46:14.34 (2000), known as Ultra-Deep Field (UDF) ACS 07675, or GOODS-CDFS-MUSIC 11517 (e.g. Grazian et al. 2006). Our earlier analysis of this object (Rauch et al. 2011, hereafter Paper I), based on the discovery spectrum taken with LDSS3 on the Magellan-II telescope, showed an area of complex, anisotropic Ly α emission continuously traceable out to about 35 h_{70}^{-1} proper kpc to the South of the galaxy. We interpreted the blueshift of the main, linear stretch of Ly α emission with respect to the damped Ly α absorption (DLA) by the galaxy, and the fact that the DLA partly absorbs the emission, as evidence for backside infall of a filamentary structure of gas on to the galaxy. The fact that the filament is hardly tilted or distorted in velocity space suggests a velocity that is more or less constant when approaching the galaxy, which is predicted by some theoretical studies of streams in the cold accretion scenario (e.g. Goerdt & Ceverino 2015, and references therein). The large extent and simple velocity structure of the filament, together with its extreme asymmetry (it is visible only to one side of the galaxy) suggested that it may be gas fluorescing in response to ionizing radiation escaping anisotropically from the galaxy itself.

The earlier paper was concerned mainly with the Ly α emission and the gaseous environment. Here, we extend our analysis to include a closer look at the observational properties of the underlying galaxy, as they appear in the broad-band images taken with the *HST* ACS camera by the *Hubble Ultra Deep Field* project (*HUDF*; Beckwith et al. 2006). The present study will use these imaging data to shed light on our original interpretation of the nature of the Ly α emitter, and constrain the properties of the underlying flows of gas and stars. We will argue that some of the broad-band emission seen in the *HST* images can be interpreted as extragalactic nebular continuum emission, and discuss several physical explanations, in particular the fluorescence of gaseous in- and outflows illuminated by ionizing photons escaping from the galaxy.

2 OBSERVATIONS

2.1 Appearance of the Ly α emission

Fig. 1 shows the two-dimensional LDSS3 spectrum around the Ly α emission line, together with several one-dimensional, 3-pixel wide (3 $\times$ 0.188 arcsec) extracted spectral cuts. Two main regions of emission can be seen, a more compact one to the right (red) side that we called the 'Red Core' in Paper I, which, aside from its spatial asymmetry, looks similar to a standard Ly α halo (e.g. Rauch et al. 2013a). To the left and blueward of the Red Core extends a triangular region (the 'Blue Fan'). The blue end of the Blue Fan is occupied by a filamentary ridge of emission (the 'Filament', see also 2). In the original analysis, the filamentary structure appeared to consist of two well-separated ridges which could be traced out to several tens of kpc, but re-reducing the data with an improved wavelength registration now shows these ridges closer together and merging into one sharper structure beyond 7 kpc away from the galaxy. The total fluxes in the filament and the red core are comparable. At distances along the slit beyond 10 kpc from the galaxy, the flux density in the filament begins to dominate over that of the red core. The spectral cuts show that – except perhaps for the central cut – the filament and the red core are narrower in velocity space than predicted for a light source filling the slit (see the resolution profile near the bottom cut in the figure), suggesting that they are smaller in the E–W direction than the 2 arcsec slit-width.

2.2 Ly α emission and the underlying galaxy

Further constraints on the nature of the emitter can be obtained from the publicly available *HST* ACS images recorded by the *HUDF* project (Beckwith et al. 2006). Fig. 2 shows how the Ly α emission and the underlying galaxy relate to each other. The 2D spectrum of the Ly α emission line is given in the leftmost panel, and the ACS *V*- (*F606W*) and *I* (*F775W*)-band images of the underlying galaxy UDF-ACS-07675 in the central and right panels, respectively. For better visibility, the broad-band images are somewhat

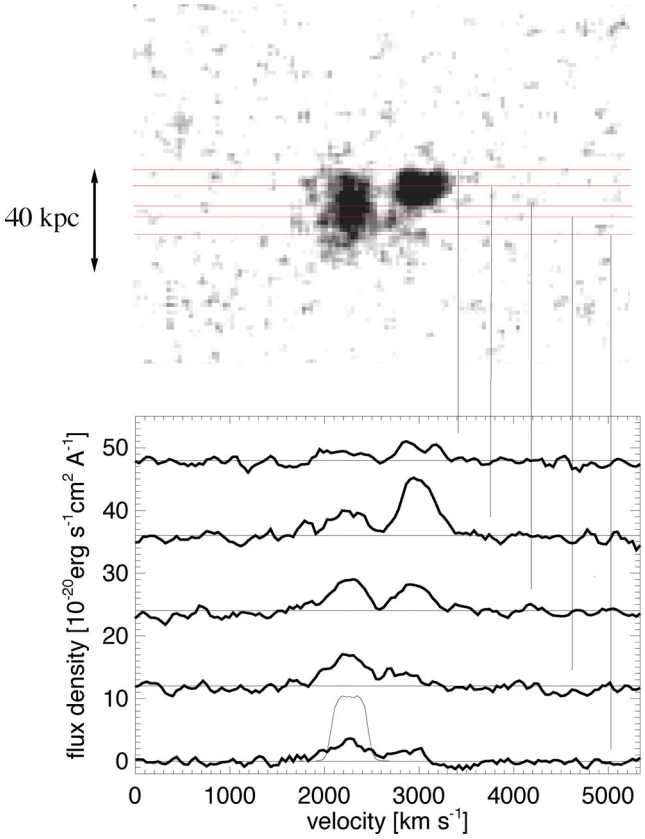

Figure 1. Spectral slices through the two-dimensional spectrum of the Ly α emitting region. The dispersion runs from left to right (blue to red), the spatial direction along the slit from bottom (South) to top (North). The solid curves in the bottom half of the plot are 3 pixel wide (0.56 arcsec) spectra extracted along the parallel thin lines shown in the top panel. The top-most spectrum approximately corresponds to the position (along the slit) of the galactic continuum, which cannot be seen here because of the DLA absorption trough. The thin-line flat-topped profile in the bottom spectrum shows the spectral resolution profile for a line source filling the slit (from a HeNeAr calibration lamp).

enlarged compared to the spectrum. Spectrum and images are lined up in the direction along the slit (N–S) to make the faint spectral continuum trace (not visible here but indicated by a dashed line) coincide with the centroid of the emission in the *V* band. For illustrative purposes, the outlines of the blue (solid) and red (dashed) Ly α emission components are arbitrarily shifted on to and overplotted on the *V*-band image, with the contours representing a Ly α flux density at approximately the 5×10^{-20} erg cm^{-2} s^{-1} Å^{-1} level. Because the contours are taken from a spectrum, they are a combination of spatial and velocity structure, and thus the precise spatial alignment with the image along the dispersion direction and its spatial width in the dispersion direction is uncertain.

It can be seen that the two Ly α components occur only to the South of the galaxy. The *V*-band image (centre of Fig. 2; for a detailed view see Fig. 4) shows tentacles of emission emerging from the galaxy in the general direction of the Ly α emission, and an additional tail with a distinct head extending about 1.5 arcsec to the right (i.e. West). The flux in the tentacles is statistically significant at the 7.7 (*V* band), 4.7 (*I* band) and 5.5 (*z* band) σ levels, and the flux in the tail is a 4.9 (*V* band) and 4.3 (*I* band) σ detection.

2.3 Appearance of the immediately galactic neighbourhood

An image of the larger scale environment of the galaxy is given in Fig. 3. A 12.6 × 8.7 arcsec (94 × 65 proper kpc) *HUDF V*-band image shows the main $z = 3.344$ galaxy close to the centre. The vertical straight lines are the outlines of the N–S oriented slit used to obtain the spectrum in Figs 1 and 2. The tilted straight lines show a second slit position that was used for auxiliary spectroscopy to probe the redshifts of an apparent filament of galaxies. This second spectrum, with a total exposure time of 66 000 s is not shown here, as it is of much poorer quality than the main spectrum. It nevertheless shows two spots with Ly α line emission at virtually the same redshift as the main Ly α emission complex. The spatial positions along the slit of these two emission spots are denoted by 'LyA' and 'LyB', and by two arrows marked with 'zsp = 3.3 Ly α'. The remaining numbers in the image are photometric redshifts (from Coe et al. 2006) within $\Delta z = \pm 0.5$ of the spectroscopic Ly α emission redshift 3.344 of the main galaxy. At the very faint magnitudes of these galaxies, the uncertainty of the published redshifts in this sample is large enough that all of them could plausibly be residing at the same redshift. In addition, the morphological similarity of several objects to the ones having spectroscopic Ly α redshifts, or to ones having photometric redshifts closer to the spectroscopic one suggests that we treat these galaxies as candidate redshift = 3.3 objects, although we should expect false positives and negatives in this sample. The linear grouping of the spectroscopic Ly α *A* and *B* $z = 3.3$ redshifts with at least four and possibly more galaxies with similar redshifts ($z = 2.926, 3.883, 3.366, 3.683$) situated under the second slit, and the existence of another linear group to the West ($z = 3.734, 3.720, 2.921$) are suggestive of some larger scale structure coarsely aligned with the NNW–SSE opening cone of the tentacles of the main galaxy. The picture is made more complicated by the presence of several other candidates near the S bottom of the image ($z = 3.207, 3.428, 3.130, 3.710, 3.348$), of which the brightest one (with $z = 3.428$), consists of three knots of emission also aligned in the general direction towards the main galaxy. This object has a SFR of 43.9 $M_\odot$ yr^{-1} (Xue et al. 2010), about ten times the value of the main galaxy. It is about 3.8 arcsec away from the edge of the slit, but it could conceivably have contributed, perhaps through fluorescence, to the Ly α emission covered by the slit.

2.4 Detailed properties of the galaxy

Closer inspection of the galaxy itself in *HST* broad-band images reveals a number of additional interesting clues to the nature of this object. An enlarged image of the galaxy is given in Fig. 4. The *V*-band image (left-hand panel) shows at least five tentacular features stretching SSE between 4 and 6 kpc from the centre of emission (indicated in the *I*-band image (right-hand panel) as a white dot). A crude, hand-drawn contour outline of the tentacles in the *V*-band image, overlaid on the *I*-band image, shows some of the appendages (the knot between 1 and 2, and the features 4 and 5 and the 'tail' to the right) to be present in the *I* band as well. The presence of emission in both filters implies that we are seeing some form of continuum radiation. The tail to the right looks like a typical tidal feature, e.g. a dwarf galaxy that may have passed through the main object, with its flux peaking at the end of the structure. The tentacles to the South look more unusual, on account of their number, their similar length and surface brightness, and the fact that their flux is not peaked at the end of the tentacles, as one might naively expect if they were a swarm of tidal stellar features.

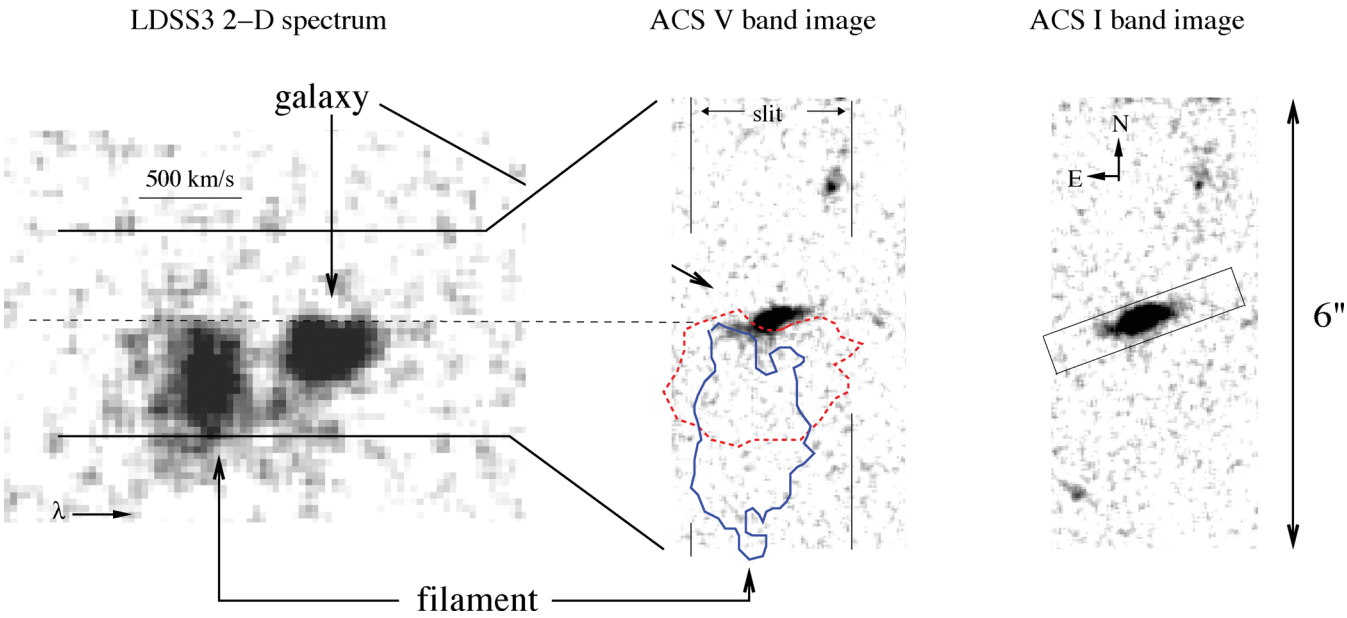

Figure 2. Left-hand panel: two-dimensional spectrum of the Ly α emission line, with the spectral dispersion horizontally, and the spatial direction along the slit vertically. The spatial position of the continuum is indicated by the thin dashed horizontal line. As argued in Paper I, the triangular emission fan encompasses a compact, red-dominant Ly α emission peak presumably arising in the direct vicinity of the galaxy, and a blue-shifted, 'filament' (or multiple unresolved filaments) of emission that is far more spatially extended along the slit. Middle panel: *F606W* image of UDF ACS 07675. Note the change in spatial scale between spectrum and image. Faint emission in both bands extends South (bottom) and West (right) of the galaxy. The two thin vertical lines indicate the slit edges. The thin solid (blue) contour in the middle panel delineates approximately the 5×10^{-20} erg cm^{-2} s^{-1} Å^{-1} flux density level of the spectrum of the 'filament'; the dotted (red) contour corresponds to the redder ('red core') emission region. Both were scaled and overplotted on the image to demonstrate the relative spatial extents of the Ly α and the continuum emission in the direction along the slit (N–S). This is for illustrative purposes only, as the E–W width and alignment between the flux density contours (which are observed in wavelength space) and the broad-band image is uncertain beyond the requirement that both have to have arisen from a region within the projected footprint of the spectrograph slit. The rightmost panel shows the *F775W I*-band image with the rectangular extraction aperture used for the spatial cut in surface brightness shown below in Fig. 5.

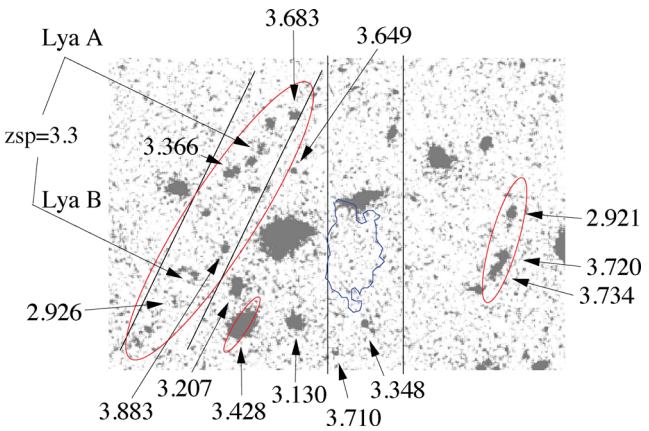

Figure 3. 12.6 × 8.7 arcsec *HUDF V*-band image of the larger scale environment of the main Ly α emitting galaxy. North is up and East to the left. The position of the two slits is shown. The positions (along the tilted slit) of two new Ly α emitting spots detected at the same redshift as the main Ly α emitting galaxy ($z = 3.344$) are given as 'Lya A' and 'Lya B'. The other numbers are photometric redshifts (from Coe et al. 2006) for objects with $z = 3.344 \pm 0.5$. The red ellipses mark structures tentatively suggestive of alignment with the central galaxy and its Ly α emitting 'filament' (thin blue contour).

The left-hand panel of Fig. 5 shows the relative surface brightness along a linear cut with a position angle of -20°, approximately aligned with the direction of largest extent of the galaxy. The flux was determined by adding up the pixel fluxes perpendicular to and across a width of 0.57 arcsec in a rectangular extraction window aligned with this direction (its outline is shown in the rightmost panel of Fig. 2). It can be seen that the flux is sharply peaked and increasingly asymmetric going blueward from z via I to the V band, giving the galaxy its distinct tadpole appearance. Aside from the peak, the bluest colours occur between -6 and -2 kpc, i.e. they arise in the small-scale tentacles.

3 PHYSICAL ORIGIN OF THE FILAMENTARY CONTINUUM EMISSION

The origin of the continuum radiation detected in the broad images of the tentacular region is not immediately clear. The standard expectation, that this is just another case of stellar continuum emission, is not necessarily the only explanation. Given the location of the galaxy in a large and obviously gas-rich Ly α emitting environment, and the unusual shape and relatively homogeneous surface brightness of the tentacles we may be seeing an extragalactic incidence of nebular continuum emission of some sort. Thus, we shall discuss three main alternative astrophysical sources for the observed continuum radiation: (1) a stellar continuum; (2) collisional excitation two-photon continuum; and (3) a fluorescent recombination spectrum, emitted in response to ionizing radiation from stars in the galaxy.

3.1 Stellar continuum radiation

The broad-band colours of the tentacle region can be well represented by the continuum emission from a conventional stellar population. Fitting STARBURST99 (Leitherer et al. 1999) galactic

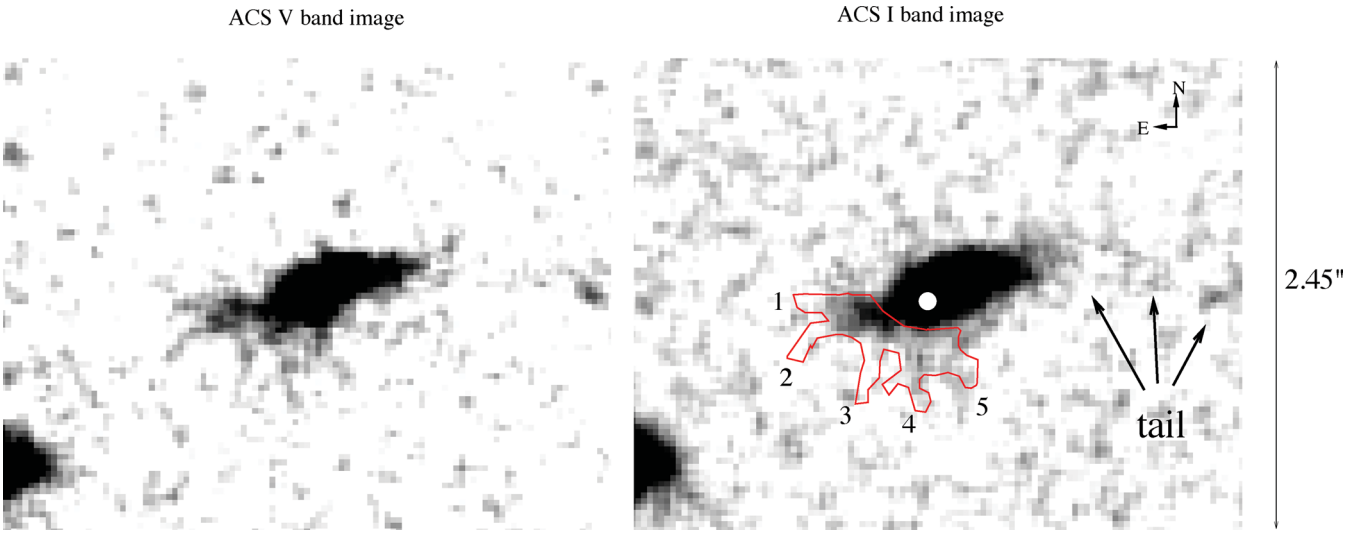

Figure 4. Enlargement of the *V* and *I*-band images, showing several tentacles of emission to the immediate bottom-left (South-East), and a longer tail extending for about ∼1.5 arcsec (11.5 kpc) to the (right) West, ending in a faint knot at the right edge of the images. The white spot in the right-hand panel shows the position of peak *V*-band emission. The contours in the *I*-band image give the outline of the tentacular *V*-band structures, to aid cross-identification with the *I*-band image. The presence of common emission features in both bands (the knot between 1 and 2, and the filaments 4 and 5; and the long tail) suggests the presence of continuum emission in these structures.

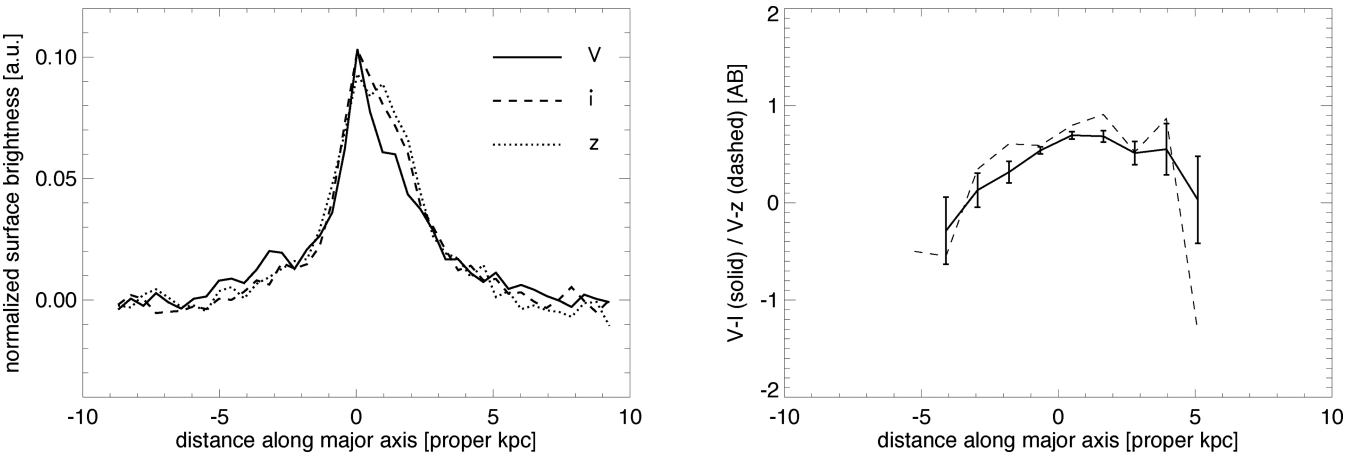

Figure 5. Relative surface brightness per pixel along a direction aligned with the approximate position angle of −20° of the galaxy. The flux was determined by adding up the pixel fluxes perpendicular to and across a width of 0.57 arcsec in an extraction window aligned with this direction. The origin of the coordinates was arbitrarily placed near the brightness peak. Left-hand panel: normalized surface brightness in three bands; right-hand panel: spatially smoothed $V-I$ (solid) and $V-z$ (dashed) colours versus distance along the cut. To avoid confusion, only the $V-I$ errors are plotted.

spectra of instantaneous starbursts of different ages to the observed *HST B*-, *V*-, *I*-, *z*-, and*Y*-band images (with the additional *Y* band taken from the CANDELS survey; Koekemoer et al. 2011), the best fit (with a reduced $\chi^2_\nu = 0.85$) was achieved with a stellar population with age of 6×10^7 yr (top panel in Fig. 6).

3.2 Collisionally excited two-photon continuum

Alternatively, the continuum emission could represent the two-photon continuum emitted in competition to Ly α line radiation (e.g. Dijkstra 2009, and references therein) during either recombination or collisional excitation of hydrogen. With temperatures and densities characteristic of the IGM close to high-redshift galaxies ($T \sim$ a few $\times 10^4$ K, $n \sim 0.1-1$ cm^{-3}), collisional excitation of Ly α emission may be an important indicator of gas cooling in galactic potential wells (e.g. Haiman et al. 2000; Dijkstra & Loeb 2009; Goerdt et al. 2010; Faucher-Giguère et al. 2010). A significant fraction of the gravitational energy will be carried away by H I two-photon continuum radiation.

Is it plausible that we may be seeing a combination of Ly α and two-photon continuum emission in the *HST* ACS broad-band images? To test this possibility, we have designed a toy model to study the expected emission with the CLOUDY code (Ferland et al. 2013). The width of the tentacles is spatially unresolved; we take them to be cylindrical, and with radius of $R = 500$ pc and a typical length of $L = 3.5$ kpc. For the CLOUDY simulation, we replace the resulting gas volume by a sphere of equal volume. This is justifiable as we are only testing for the overall viability of creating the observed continuum emission through collisional excitation, and any geometry will be optically thin for two-photon continuum (but optically thick for Ly α photons, the radiative transfer of which we cannot model anyway).

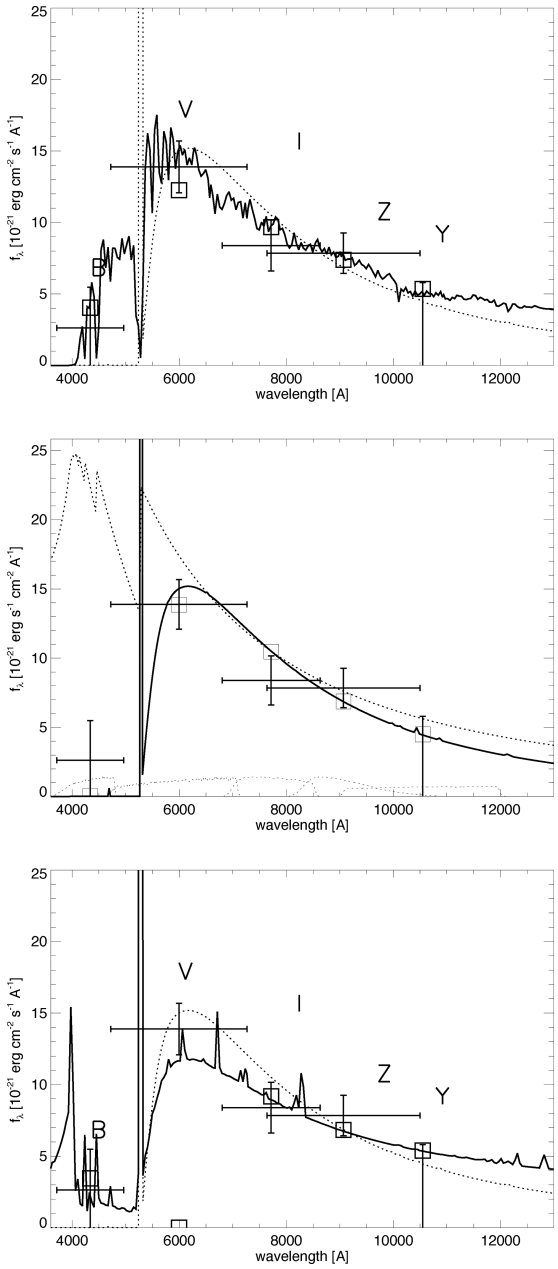

Figure 6. Spectra of three alternative models for the broad-band colours of the tentacles. The models are trying to reproduce the emission as coming from either: (1) a starburst stellar continuum (top); (2) collisionally excited cooling radiation (centre); or (3) a fluorescent recombination spectrum of gas exposed to an ionizing stellar continuum (bottom). The data points with error bars represent the observed fluxes in the various bands from within the contour shown in the right-hand panel of Fig. 4. The little square boxes give the integrated fluxes passing through the same filters for the model spectra. The top panel shows the spectrum of a 6×10^7 yr old starburst from STARBURST99 (solid line). The central panel shows the spectrum of collisionally excited gas from a CLOUDY model described in the text (solid line; also overplotted for comparison as a dotted line in the top- and bottom panels). The dotted line in the central panel shows a continuum of the form $f_\lambda \propto \lambda^{-\beta}$, with $\beta = 2$ for illustration. The curves at the bottom of the central panel are of the transmission curves of the *HST* filters (arbitrary units). The bottom panel shows a fluorescent recombination spectrum produced by ionizing radiation from a starburst. All spectra were attenuated by the appropriate Ly α forest absorption (Inoue et al. 2014). In the central panel, the *V* band was fit separately to account for the unknown Ly α escape fraction. In the bottom panel, no fit was attempted for the *V* band.

The gas in the spherical toy model is placed at a constant temperature of 18 000 K, close to the temperature that maximizes collisional excitation of H I. Such a constellation may be found in a cooling stream, where the temperature is kept up by a steady supply of gravitational energy by the infalling matter. A photoionizing UV background according to Haardt & Madau (1996) is adopted although the presence of the extragalactic UV background makes little difference. A metallicity typical for the high-redshift IGM ($Z = 10^{-2.8}\,Z_\odot$; e.g. Schaye et al. 2003; Simcoe, Sargent & Rauch 2004) was assumed for the gas, but the exact metallicity value is not very important. Even increasing the metallicity in the gas to solar values would increase the cooling rate by only about 20 per cent.

To determine the cooling flux, we fit the fluxes observed within the tentacles' contour in the *B*-, *V*-, *I*-, *z*-, and *Y*-bands (omitting the *V* band that may contain the Ly α line) with cooling radiation spectra from CLOUDY, using the gas density as the only free parameter. A density of 0.75 cm^{-3} gives the best fit, with a reduced $\chi^2_\nu = 1.66$ (Fig. 6, central panel). Having determined the strength of the continuum and the intrinsic Ly α flux (1.3×10^{-16} erg cm^{-2} s^{-1}) this way, we fit the *V* band separately, now treating the fraction of the intrinsic Ly α that is observed within the tentacular contour, $f_{\rm tent}^{{\rm Ly}\alpha}$, as the free parameter. It is found that 18.4 per cent of the *V*-band flux need to be supplied by Ly α line emission, corresponding to $f_{\rm tent}^{{\rm Ly}\alpha} = 6.2 \pm 4.4$ per cent. The error comes from the uncertainty in the observed *V*-band flux only and is thus a strict lower limit to the actual uncertainty. Even given the large uncertainty, we can say the majority of flux in the *V* band must come from the two-photon continuum. The small contribution of Ly α to the total emission directly from the volume of the tentacles into the observer's line of sight is quite expected because Ly α is likely to get scattered out of the tentacles before being able to escape the galactic halo, whereas the two-photon emission emerges straight from the source into our line of sight. Under the above conditions, the gas is mostly ionized (neutral fraction 13 per cent). However, if contained in tentacular tubes with the above dimensions, the gas remains self-shielded, with a minimum H I column density $N_{\rm H\,I} = 1.5 \times 10^{20}\,\frac{R}{500{\rm pc}}\,{\rm cm}^{-2}$.

The intrinsic Ly α flux (1.3×10^{-16} erg cm^{-2} s^{-1}) from cooling in the filaments overproduces the total observed flux (2.45×10^{-17} erg cm^{-2} s^{-1}, suggesting an overall apparent escape fraction for Ly α, $f_{\rm esc}^{{\rm Ly}\alpha} = 0.19$, if all the flux in the system is produced through this channel, or about half that if only the flux in the red core is. Apparent escape probabilities considerably less than unity are not unusual (e.g. Atek et al. 2009; Blanc et al. 2011) and may be due to destruction of Ly α photons by dust, anisotropic emission, or aperture losses.

At the optimal temperature of 18 000 K the tentacle gas, for the adopted volume and density, undergoes collisional cooling at the rate of $\mathrm{d}E_{\rm cool}/\mathrm{d}t = 2.3 \times 10^{43}$ erg s^{-1}. This is very similar to the total gravitational heating rate expected for a galaxy with a total mass of $10^{12}\,{\rm M}_\odot$ at this redshift (1.6×10^{43} erg s^{-1}; Goerdt et al. 2010; see also Faucher-Giguère et al. 2010).

An indirect estimate of the halo mass can be obtained from the spectral energy distribution. Using the MAGPHYS code (da Cunha, Charlot & Elbaz 2008) with the information obtained from bands ACS *F*435*W*, ACS *F*606*W*, ACS *F*775*W*, ACS *F*850*LP*, NICMOS *F*110*W* and NICMOS *F*160*W*, and allowing for the presence of dust gives a stellar mass of $2.4 \times 10^9\,{\rm M}_\odot$, corresponding to a typical halo mass of $\sim 7 \times 10^{11}\,{\rm M}_\odot$ according to theoretical stellar/halo mass relations (e.g. Moster et al. 2010). In other words, the total gravitational energy gained by cold accretion in the halo of the galaxy is of the same order of magnitude as the cooling rate required to explain the continuum flux in the tentacles as H I two-photon

cooling radiation. This result requires that most the gravitational energy is re-radiated at small radii by the tentacles, which is not implausible. In the simulations by Rosdahl & Blaizot (2012), half of the total cooling energy for haloes of similar masses is emitted at radii of less than 10 kpc. A possible problem with the interpretation of the tentacular flux as cooling radiation arises from the relatively high SFR suggested by the expected mass accretion rate for a $\sim 7 \times 10^{11} \mathrm{M}_{\odot}$ halo ($M_{\rm cold} \sim 100\,\mathrm{M}_{\odot}\ \mathrm{yr}^{-1}$; e.g. Goerdt et al. 2010) and the more measly observed SFR of 4.1 $\mathrm{M}_{\odot}\ \mathrm{yr}^{-1}$ (derived from MAGPHYS; this is a somewhat higher value that the 1.7 $\mathrm{M}_{\odot}\ \mathrm{yr}^{-1}$ we had estimated in Paper I, then based solely on the *F*606*W* flux before extinction correction). If star formation is efficient and most of the accreted gas ends up in stars, $M_{*} \approx M_{\rm cold}$, one would obtain a SFR 25 times larger than the observed 4.1 $\mathrm{M}_{\odot}\ \mathrm{yr}^{-1}$. We are forced to conclude that either star formation in the present case is currently highly inefficient, or that the accretion rate and/or the total mass of the galaxy are much smaller. In the latter case, a galaxy mass commensurate with the observed SFR would be $2.5 \times 10^{10} \mathrm{M}_{\odot}$. The corresponding gravitational heating rate for such a halo (Goerdt et al. 2010, equation 7) would then be almost three orders of magnitude smaller than required to produce the observed cooling continuum. Of course, any of those arguments are applicable only in a statistical sense.

3.3 Fluorescent recombination emission

Alternatively, nebular continuum emission can arise when H I gas fluoresces in response to ionizing radiation from either stars or an AGN (for discussions; see e.g. Cantalupo et al. 2005; Kollmeier et al. 2010). Both the energetics and the shape of the emerging spectrum depend on a considerable number of parameters, including the distance of the gas from the sources, the column density along the line of sight and between source and irradiated gas cloud, the ionizing spectrum, the relative prominence of collisional versus photoionization excitation and the metallicity of the gas, so we can at best check the plausibility of this process. The result of one particular realization is shown in the bottom panel of Fig. 6. Using CLOUDY, we model the 'reflected' fluorescent radiation when bouncing into our line of sight off a gas cloud irradiated by a 5×10^{6} yr old starburst. Again omitting the *V* band from the fit (because of its susceptibility to the Ly α escape fraction), we obtain a fit to the observed continuum colours in the tentacles with $\chi^2_{\nu} = 0.85$, as good as the fit with the stellar continuum above. The somewhat better agreement for the fluorescent case as compared to the earlier collision excitation case is owed to the production of diffuse H I ionizing continuum emission (which was absent in the case of collisional excitation). However, the relative strength of the actually observed nebular ionizing continuum may depend strongly on the position of the gas clouds relative to the ionizing source and the observer, so the better fit for the fluorescent case may be fortuitous. Other differences between the fluorescent spectrum and the mainly two-photon continuum of the collisional case are the presence of metal recombination lines (which are weak here as we assumed the mean metallicity of the IGM at $z \sim 3$, $Z = 10^{-2.8} \times \mathrm{Z}_{\odot}$ (e.g. Schaye et al. 2003; Simcoe et al. 2004), and a shallower continuum slope in the red due to the fluorescent Balmer continuum.

Explaining the tentacular continuum as fluorescent would be consistent with our earlier proposal that the extended Ly α emission itself is due to fluorescence induced by ionizing stellar photons that have escaped the galaxy. The absence of a detectable underlying stellar population within the footprint of the Ly α filament and the lack of surface brightness gradients expected, if Ly α photons were 'random-walking' outward from an optically thick galaxy make this the most plausible scenario.

We cannot rule out the presence of an AGN, which would be expected to leak photons below the Lyman limit and could lead to similar, large-scale Ly α emission, but, as argued earlier, the number of ionizing photons produced by the observed stars is sufficient to explain the observed Ly α flux, and the peculiar morphology of the galaxy certainly suggests that star formation is the relevant process here.

4 OUTFLOWS VERSUS INFLOWS – PHYSICAL NATURE OF THE TENTACLES

The astrophysical nature of the tentacles cannot be decided just from knowing the origin of the tentacles emission (i.e. stellar versus gas cooling versus photoionization), and additional morphological or kinematic information is required.

We shall briefly discuss four scenarios that may be capable of producing galaxies with tentacles as observed:

(1) *Galactic winds*. Even though the large-sale filament may be infalling gas, this does not have to be the case for the smaller tentacles, which have some morphological resemblance to gaseous filaments seen in galactic winds (e.g. Veilleux, Cecil & Bland-Hawthorn 2005). Although the total SFR of 4.1 $\mathrm{M}_{\odot}\ \mathrm{yr}^{-1}$ is moderate, the SFR density should be enough to drive a galaxy wide wind (according to the criterion given by Heckman 2002). Somewhat surprisingly for an outflow, the tentacles appear strictly on one side, and not in the bipolar pattern expected. Besides, they seem to converge on or emerge from a location slightly in front of the galaxy (in the direction of the Ly α emission) that does not agree with the luminosity peak (and presumed peak of star formation). If the tentacles were mainly illuminated by fluorescence, such an asymmetric pattern with a wind cone visible only on one side would be expected (with the other cone present but not illuminated), and recombination could be sufficient to produce the observed continuum. Cooling radiation from dense, cold, entrained matter appears less likely as it would arise equally strong in both wind cones. Star formation triggered by some types of outflows, e.g. galactic superbubbles (Oey et al. 2005) and AGN outflows (e.g., Van Breughel et al. 1985; Rauch et al. 2013b) has been observed, but the filamentary structures sometimes seen in galactic winds do not seem to be populated with newly formed stars, so a tentacular structure of stars may be an unlikely outcome for a wind scenario. Finally, as can be seen from the spectral cuts in Fig. 1, beyond the innermost few kpc the Ly α emission filament remains more or less perpendicular to the dispersion direction, which means that the gas is neither accelerating nor decelerating, as may be expected for various wind models. On the other hand, velocity gradients would be hard to see if the wind and the orientation of the tentacles were largely perpendicular to the line of sight. In short, the possibility that the tentacles arise in a galactic wind cannot be ruled out, but it is not obvious either.

(2) *Ram-pressure stripping*. Ram-pressure stripping may create linear filaments of new star formation downwind from the stripped galaxy, which would indeed explain the occurrence of emitting tentacles strictly on only one side of the galaxy. However, the stripped contrails observed so far at lower redshifts are generally parallel to each other, following hydrodynamic streamlines away from the galaxy (e.g. Hester et al. 2010; Ebeling, Stephenson & Edge 2014), in contrast to the highly focused bundle of tentacles observed in the present case. Thus, ram-pressure stripping of the galaxy itself when moving with respect to the surrounding IGM appears an unlikely explanation.

(3) *Galactic wakes forming behind satellite haloes when passing through the main halo*. Accretion streams in the cosmic web consist not just of gas but of galactic haloes as well and must be exposing the main galaxy to a constant bombardment with satellite haloes. These objects, as far as they are not getting completely destroyed on their passage through the galaxy, will be tidally and pressure-stripped and may re-emerge postpassage with a new tail of ripped-out interstellar medium (ISM) from the galaxy, with trajectories bent by the gravitational potential of the main galaxy. These processes are seen in cosmological simulations (e.g. Agertz et al. 2011; Rosdahl & Blaizot 2012; Keres et al. 2012). While the occurrence of satellite tails is difficult to observe at the level of individual high-redshift galaxies, they must be common and play an important role in the metal-enrichment of galactic haloes at high z. The 'tail' to the West (right in Fig. 4) of the galaxy is almost certainly of this kind. The tentacles look very similar to multiple tails passing through the lowest mass halo shown by Rosdahl & Blaizot (2012) in their fig. 10. The similar morphology, however, does not necessarily require that the emission mechanisms are the same. The detectable tentacular emission in the Rosdahl & Blaizot simulated halo appears dominated by gravitational cooling radiation, but in our case the tentacles could just as well be illuminated by fluorescence from the galaxy.

(4) *Cold accretion streams connecting to the galaxy.* The tentacles may be actual cold accretion, i.e. inflowing gas conduits connecting the large scale accretion filament to the ISM of the galaxy. When the relatively wide (kpc scale) IGM accretion streams converge on a galaxy, they must get pinched to a much smaller diameter by the ambient pressure of the galactic halo. This compression and shrinking of the infalling filaments is seen in some simulations (e.g. Agertz et al. 2011). We can speculate that the compression may enhance cooling radiation and may even induce star-formation in the gas while in final descent on to the galaxy. If these processes take place, they may lead to the formation of one or several bright knots of emission at the convergence of the tentacles, and may explain the general lining up of these tentacles with the direction of the large scale filament that we see in Ly α emission, and the large-scale distribution of galaxies further out.

5 CONCLUSIONS

We have discussed the nature of an asymmetric Ly α emitter associated with a peculiar star forming galaxy. As described in Paper I, spatial distribution and kinematics of the Ly α emitting gas suggest a picture of gas falling into a galaxy while being lit up by ionizing radiation escaping from that object. Based on an examination of *HST* imaging data, the underlying galaxy exhibits a 'tadpole' shape in the *V* band, with a hotspot of blue continuum emission on the edge facing the direction of the massive Ly α emission. The galaxy further shows a stretch of continuum light likely to represent a tidally or pressure-stripped passing satellite galaxy, and several sharply delineated tentacles of continuum emission protruding to about 5 kpc from the galaxy in the direction towards the Ly α emission. The morphology of the tentacles and their similar spatial range and surface brightness suggest that we are seeing extragalactic nebular emission dominated by H I two-photon continuum emission (as opposed to star light). The broad-band colours and the energy requirements are consistent with collisionally excited cooling radiation powered by potential energy of gas falling into a galaxy of this type. However, the observed current SFR of the galaxy falls short of matching the predicted mass accretion rate by a factor of $\sim$25. Perhaps more compellingly, we may be seeing recombination radiation from gas fluorescing in response to ionizing radiation escaping from the galaxy. As argued in Paper I, this explanation is energetically compatible with the observed star formation. It would also most easily explain the presence of Ly α emission in the large-scale filament, tens of kpc away from the galaxy as being lit up directly by a beam of escaping ionizing radiation. Alternatively, in the absence of any discernable local sources residing in the Ly α emitting region, its Ly α would have to be either propagated by scattering through an optically thick halo all the way from the galaxy, leading to an (unobserved) strong gradient in the surface brightness as a function of distance or be produced by cooling at distances from the galaxy as large as several tens of kpc, where the density is likely to be lower than the $\sim$1 cm^{-3} required to produce detectable cooling radiation in the current case.

The emission mechanism alone (nebular emission, either collisional or recombination continua) is insufficient to uniquely identify the astrophysical setting of the tentacular phenomenon. The tentacles could be features of a galactic windblown by star formation that is triggered by the infalling gas. Alternatively, theoretical infall scenarios predict cold stream filaments converging at galaxies which look very similar to the observed structures. A third explanation, within the same accretion scenario, might envisage infalling dwarf satellite haloes piercing the ISM of the main halo and pulling out dense filaments of gas, which could be seen either while cooling or again when being exposed to ionizing photons.

In any case, the combined evidence from the elongated gas distribution, the kinematics of the gas, the large scale environment, the apparent hotspot of star formation, the nebular continuum emission, the likely escape of ionizing photons and the presence of at least one interacting satellite halo appears to be intriguing evidence for an instance of a galaxy undergoing accretion of gas and smaller haloes from the IGM. Until it becomes instrumentally possible to detect the Ly α glow of the IGM in response to the UV background, the search for galaxies that illuminate themselves through some fortuitous release of Ly α or ionizing radiation into their environment may provide our main direct insights into the in- and outflows of gas. Searches for asymmetric Ly α haloes or offsets between stellar populations and Ly α emission may reveal further objects where the escape of ionizing radiation can be studied.

The detection of extragalactic two-photon continuum emission in space-based, broad-band images of galaxies flagged by asymmetric Ly α emission may become a new tool for probing the gaseous environment of high-redshift galaxies. Unlike Ly α or other resonance lines, the two-photon continuum emission is not spatially blurred as it is emitted under optically thin conditions, suggesting that it can be used to image small-scale features in the IGM at much greater spatial resolution.

ACKNOWLEDGEMENTS

This paper includes data gathered with the 6.5 metre Magellan Telescopes located at Las Campanas Observatory, Chile. We thank the staff of Las Campanas Observatory for their help with the observations. This paper is based partly on observations made with the NASA/ESA *Hubble Space Telescope*, and obtained from the Hubble Legacy Archive, which is a collaboration between the Space Telescope Science Institute (STScI/NASA), the Space Telescope European Coordinating Facility (ST-ECF/ESA) and the Canadian Astronomy Data Centre (CADC/NRC/CSA). This research has made use of the NASA/IPAC Extragalactic Database (NED), which is operated by the Jet Propulsion Laboratory, California Institute of Technology, under contract with the National Aeronautics and

Space Administration. MR was supported by grant AST-1108815 from the National Science Foundation. This work was supported by the ERC Advanced Grant 320596. The Emergence of Structure during the epoch of Reionization.

REFERENCES

Adelberger K. L., Steidel C. C., Kollmeier J. A., Reddy N. A., 2006, ApJ, 637, 74
Agertz O., Teyssier R., Moore B., 2011, MNRAS, 410, 1391
Atek H., Kunth D., Schaerer D., Hayes M., Deharveng J. M., Östlin G., Mas-Hesse J. M., 2009, A&A, 506, 1
Beckwith S. V. W. et al., 2006, AJ, 132, 1729
Blanc G. A. et al., 2011, ApJ, 736, 31
Bunker A., Smith J., Spinrad H., Stern D., Warren S., 2003 Ap&SS, 284, 357
Cantalupo S., Porciani C., Lilly S. J., Miniati F., 2005, ApJ, 628, 61
Cantalupo S., Lilly S. J., Porciani C., 2007, ApJ, 657, 135
Cen R., Zheng Z., 2013, ApJ, 775, 112
Coe D., Benitez N., Sanchez S. F., Jee M., Bouwens R., Ford H., 2006, ApJ, 132, 926
da Cunha E., Charlot S., Elbaz D., 2008, MNRAS, 388, 1595
Dijkstra M., 2009, ApJ, 690, 82
Dijkstra M., Loeb A., 2009, MNRAS, 400, 1109
Dijkstra M., Haiman Z., Spaans M., 2006, ApJ, 649, 14
Ebeling H., Stephenson L. N., Edge A. C., 2014, ApJ, 781, 40
Fardal M. A., Katz N., Gardner J. P., Hernquist L., Weinberg D. H., Davé R., 2001, ApJ, 562, 605
Faucher-Giguère C.-A., Kereš D., Dijkstra M., Hernquist L., Zaldarriaga M., 2010, ApJ, 725, 633
Feldmeier J. J. et al., 2013, ApJ, 776, 75
Ferland G. J. et al., 2013, Rev. Mex. Astron. Astrofis., 49, 1
Francis P. J., Bland-Hawthorn J., 2004, MNRAS, 353, 301
Fynbo J. U., Møller P., Warren S. J., 1999, MNRAS, 305, 849
Goerdt T., Ceverino D., 2015, MNRAS, 450, 3359
Goerdt T., Dekel A., Sternberg A., Ceverino D., Teyssier R., Primack J. R., 2010, MNRAS, 407, 613
Grazian A. A. et al., 2006, A&A, 449, 951
Haardt F., Madau P., 1996, ApJ, 461, 20
Haiman Z., Spaans M., Quataert E., 2000, ApJ, 537, 5
Hayashino T. et al., 2004, AJ, 128, 2073
Heckman T. M., 2002, in Mulchaey J. S., Stocke J., eds, ASP Conf. Ser. Vol. 254, Extragalactic Gas at Low Redshift. Astron. Soc. Pac., San Francisco, p. 292
Hennawi J. F., Prochaska J. X., Kollmeier J., Zheng Z., 2009, ApJ, 693, 49
Hester J. A. et al., 2010, ApJ, 716, 14
Inoue A. K., Shimizu I., Iwata I., Tanaka M., 2014, MNRAS, 442, 1805
Keres D., Vogelsberger M., Sijacki D., Springel V., Hernquist L., 2012, MNRAS, 425, 2027
Koekemoer A. M. et al., 2011, ApJS, 197, 36
Kollmeier J. A., Zheng Z., Davé R., Gould A., Katz N., Miralda-Escudé J., Weinberg D. H., 2010, ApJ, 708, 1048
Leitherer C. et al., 1999, ApJS, 123, 3
Martin D. C., Chang D., Matuszewksi M., Morrissey P., Rahman S., Moore A., Steidel C. C., Matsuda Y., 2014a, ApJ, 786, 106
Martin D. C., Chang D., Matuszewksi M., Morrissey P., Rahman S., Moore A., Steidel C. C., 2014b, ApJ, 786, 107
Martin D. C., Matuszewski M., Morrissey P., Neill J. D., Moore A., Cantalupo S., Prochaska J. X., Chang D., 2015, Nature, 524, 192
Matsuda Y. et al., 2004, ApJ, 128, 569
Momose R. et al., 2014, MNRAS, 442, 110
Moster B. P., Somerville R. S., Maulbetsch C., van den Bosch F. C., Maccio A. V., Naab T., Oser L., 2010, ApJ, 710, 903
Oey M. S., Watson A. M., Kern K., Walth G. L., 2005, AJ, 129, 393
Ouchi M. et al., 2013, ApJ, 778, 102
Overzier R. A., Nesvadba N. P. H., Dijkstra M., Hatch N. A., Lehnert M. D., Villar-Martín M., Wilman R. J., Zirm A. W., 2013, ApJ, 771, 89
Prescott M. K. M., Momcheva I., Brammer G. B., Fynbo J. P. U., Møller P., 2015, ApJ, 802, 32
Rauch M., Becker G. D., Haehnelt M. G., Gauthier J.-R., Ravindranath S., Sargent W. L. W., 2011, MNRAS, 418, 1115 (Paper I)
Rauch M., Becker G. D., Haehnelt M. G., Gauthier J.-R., Sargent W. L. W., 2013a, MNRAS, 429, 429
Rauch M., Becker G. D., Haehnelt M. G., Carswell R. F., Gauthier J.-R., 2013b, MNRAS 431, L68
Rauch M., Becker G. D., Haehnelt M. G., Gauthier J.-R., 2014, MNRAS, 441, 73
Rosdahl J., Blaizot J., 2012, MNRAS, 423, 344
Schaye J., Aguirre A., Kim T.-S., Theuns T., Rauch M., Sargent W. L. W., 2003, ApJ, 596, 768
Simcoe R. A., Sargent W. L. W., Rauch M., 2004, ApJ, 606, 92
Steidel C. C., Bogosavljevic M., Shapley A. E., Kollmeier J. A., Reddy N. A., Erb D. K., Pettini M., 2011, ApJ, 736, 160
Trainor R. F., Steidel C. C., 2013, ApJ, 775, 3
van Breugel W., Filippenko A. V., Heckman T., Miley G., 1985, ApJ, 293, 83
Veilleux S., Cecil G., Bland-Hawthorn J., 2005, ARA&A, 43, 769
Weidinger M., Møller P., Fynbo J., 2004, Nature, 430, 999
Xue Y. Q. et al., 2010, ApJ, 720, 368
Zabl J., Nørgaard-Nielsen H. U., Fynbo J. P. U., Laursen P., Ouchi M., Kjæ rgaard P., 2015, MNRAS, 451, 2050

This paper has been typeset from a TEX/LATEX file prepared by the author.